

## **RAMAN SPECTROSCOPY OF CARBON NANOTUBES**

**Dr. SONY KUMARI**, Assistant professor (Guest faculty), Department Of Physics, Marwari College Darbhanga - [shreesony1987@gmail.com](mailto:shreesony1987@gmail.com)

### **Abstract**

A tutorial review of the use of Raman spectroscopy for carbon nanotube applications is presented here. We will discuss how to use Raman spectral features for practical purposes of controlling and characterizing nanotube properties relevant to applied materials and devices after introducing the relevant basic aspects of Raman spectroscopy of grapheme-related materials. Advanced techniques that have the potential to it are also presented how to improve the relevance of Raman spectroscopy application in the field of carbon nanotubes. Having a combination of different carbon nanotube tests, one can undoubtedly recognize, in a speedy trial, the presence of single-walled, double-walled and multiwall carbon nanotubes (SWCNT, DWCNT, MWCNT, separately). The supposed G-line is a trademark element of the graphitic layers and compares to the extraneous vibration of carbon molecules. Another characteristic mode, the D-line, is a typical sign of defective graphitic structures.

**Keyword :** Raman Spectroscopy, Grapheme, DWCNT, MWCNT, Nanotubes

### **Introduction**

Carbon nanotubes (CNT) since their revelation turned into significant logical objects of broad exploration because of their fascinating actual properties and mechanical applications. CNT have demonstrated to be a novel framework to concentrate on Raman spectra in one-layered (1D) frameworks <sup>1</sup>, and simultaneously Raman spectroscopy has given an extremely useful asset to concentrate on vibrational properties and electronic designs of CNT <sup>2</sup>, especially for portrayal of CNT's distances across, and nature of the examples. <sup>3</sup>Different carbon materials can be broke down by the Raman spectroscopy including single walled (SWCNT), double walled (DWCNT) and multi-walled (MWCNT) carbon nanotubes at the same time, sadly, quantitative assurance of each type is incomprehensible at present <sup>4</sup>.

### **Raman spectroscopy's features SWCNT and DWCNT**

The Raman spectra present various highlights being all delicate to chiral records (n,m) indicating the border vector (chiral vector), like the spiral breathing mode (RBM) where all the carbon atoms are moving in-work in the spiral heading, the G-band where adjoining atoms are moving in inverse bearings along the outer layer of the cylinder as in 2D graphite, <sup>5</sup>the dispersive problem actuated D-band and its second-order related consonant G'-band. According to the expression  $\text{RBM} \propto \frac{1}{d} + \frac{1}{d^2}$ , where is the vibration frequency and A and B are constants that vary between bundle tubes and individual tubes, the RBM appears to be more sensitive to the nanotube diameter (d). A few creators think about just the steady  $\frac{1}{d}$  in assurance of the width. A DWCNT is a type of MWCNT for which the interlayer interaction between the inner and outer nanotubes is typically regarded as turbostratic. The splitting of the G'-band that is observed in 3D graphite could be observed in armchair–armchair DWCNT and some commensurate structure could be anticipated. A small RBM

<sup>1</sup> Y.-P. Sun, K. Fu, Y. Lin, and W. Huang, "Functionalized carbon nanotubes: Properties and applications," *Acc. Chem. Res.* 35, 1096–1104 (2002).

<sup>2</sup> M. Endo, M. S. Strano, and P. M. Ajayan, "Potential applications of carbon nanotubes," in *Carbon Nanotubes* (Springer, 2007), pp. 13–62.

<sup>3</sup> A. Jorio, M. S. Dresselhaus, and G. Dresselhaus, *Carbon Nanotubes: Advanced Topics in the Synthesis, Structure, Properties and Applications*, Topics in Applied Physics Vol. 111 (Springer-Verlag, Berlin, 2008), p. 720.

<sup>4</sup> L. Hu, D. S. Hecht, and G. Gruner, "Carbon nanotube thin films: Fabrication, properties, and applications," *Chem. Rev.* 110, 5790–5844 (2010).

<sup>5</sup> DRESSELHAUS M.S., DRESSELHAUS G., SAITO R., JORIO A., *Phys. Rep.*, 409 (2005), 47.

line width (down to 0.25 cm<sup>-1</sup>) that occurs for the inner wall tube within an isolated DWCNT is another novel direction for future research <sup>6</sup>.

The distribution of the nanotubes' diameters within a particular SWCNT bundle can be determined by measuring RBM for a variety of laser energies. The G-band is hence a natural element of a carbon nanotube firmly connected with vibrations in all sp<sup>2</sup> carbon materials. The Raman line shape, which varies depending on whether the nanotube is metallic or semiconducting, is the most significant aspect of the G-band and makes it easy to distinguish between the two types. <sup>7</sup> The lower frequency component of this band, G<sub>-</sub>, is associated with vibrations that occur in the circumferential direction; the higher frequency component, G<sub>+</sub>, is associated with vibrations that occur in the G direction of the nanotube axis. Past examinations show that the previous part is reliant upon the breadth of a nanotube while the last option doesn't display this reliance in both, metallic and semiconducting nanotubes. <sup>8</sup>

At the level of a single nanotube, the Raman spectra of semiconducting and metallic SWCNT reveal both the D-band and G'-band features. Graphite's D-band is caused by scattering from a defect that disrupts the grapheme sheet's fundamental symmetry. Sp<sup>2</sup> carbons with porous impurities or other symmetry-breaking defects exhibit it. However, the second-order G'-band does not require an elastic defect-related scattering process, and for defect-free sp<sup>2</sup> carbons, Raman spectroscopy 435 can be used to characterize carbon nanotubes. The chirality and diameter of the nanotubes, as well as the laser excitation energy, are correlated with these bands. <sup>9</sup>

The introduction of the Kataura plot of the interband transitions, E<sub>ii</sub> as a function of dt for all values of (n,m) has made the analysis of all resonance Raman effects much easier. This plot shows that each pair of indices in a nanotube has a unique set of E<sub>ii</sub> transition energies, which is physically due to the trigonal warping effect of the constant energy contours for a graphite sheet.

### **Multiwall carbon nanotubes**

Concentric grapheme sheets are rolled into a cylinder with diameters of tens of nanometres to create multiwall carbon nanotubes. <sup>10</sup> The majority of the characteristic differences that distinguish the Raman spectra of SWCNT from those of graphite are not as evident in MWCNT due to the ensemble of carbon nanotubes with diameters ranging from small to very large and the large diameter of the outer tubes. When a good resonance condition is established, for instance, the RBM Raman feature associated with a small inner tube (less than 2 nm) can occasionally be observed. <sup>11</sup>

MWCNT's corresponding splitting of the G band is both small in intensity and smeared out due to the effect of the diameter distribution within the individual MWCNT and the variation between different tubes in an ensemble of MWCNT in typical experimental samples, whereas the G<sub>+</sub> "G" splitting is large for small diameter SWCNT tubes. As a result, the characteristic line shape of the G-band feature is primarily weakly asymmetric, and a peak appears close to the graphite frequency. When electrons are irradiated into MWCNT, it is to be expected that radiation exerts its most powerful influence. The appearance of radiation defects, whose presence contributes to the degradation of the nanotubes but also appears to be caused by broken bonds formed during the formation of vacancies, <sup>12</sup> may account for the feature. From Raman spectroscopy data, we

<sup>6</sup> DRESSELHAUS M.S., DRESSELHAUS G., JORIO A., SOUZA FILHO A.G., PIMENTA M.A., SAITO D.R., *Acc. Chem. Res.*, 35 (2002), 1070.

<sup>7</sup> ZHANG H.B., LIN G.D., ZHOU Z.H., DONG X., CHEN T., *Carbon*, 40 (2002), 2429.

<sup>8</sup> GRIMM D., GRÜNEIS A., KRAMBERGER C., RÜMMELI M., GEMMING T., BÜCHNER B., BARREIRO A., KUZMANY H., PFEIFFER R., PICHLER T., *Chem. Phys. Lett.*, 428 (2006), 416.

<sup>9</sup> KUZMANY H., PLANK W., HULMAN M., KRAMBERGER C., GRÜNEIS A., PICHLER T., PETERLIK H., KATAURA H., ACHIBA Y., *Eur. Phys. J. B*, 22 (2001), 307.

<sup>10</sup> ANTUNES E.F., LOBO A.O., CORAT E.J., TRAVA-AIROLDI V.J., MARTIN A.A., VERISSIMO C., *Carbon*, 44 (2006), 2202.

<sup>11</sup> KÜRTI J., KUZMANY H., BURGER B., HULMAN M., WINTER J., KRESSE G., *Synth. Metals*, 103 (1999), 2508

<sup>12</sup> RITTER U., SCHARFF P., SIEGMUND C., DMYTRENKO O.P., KULISH N.P., PRYLUTSKYY YU.I., BELYI N.M., GUBANOV V.A., KOMAROVA L.I., LIZUNOVA S.V., POROSHIN V.G., SHLAPATSKAYA V.V.,

demonstrate a straightforward method for evaluating various SWCNT physical properties in the paper.

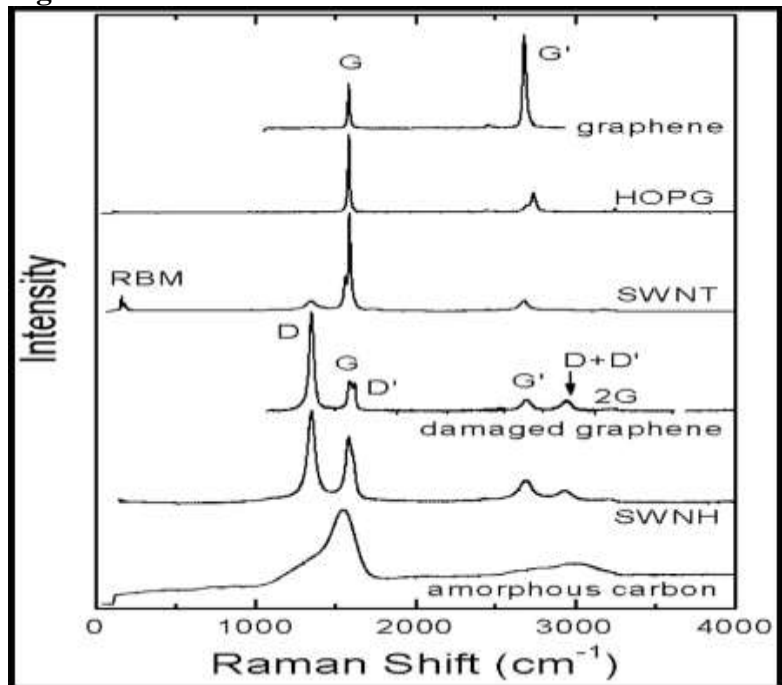
### ASPECTS GENERAL OF THE SWNTS RAMAN SPECTRA

The material responds by emitting light at the same energy (elastic scattering,  $s=i$ ) and at shifted energies (inelastic scattering,  $s \neq i$ ) when it is perturbed by monochromatic radiation, typically an incident laser of wavelength. <sup>13</sup>The Raman spectroscopy, which offers an unearthly unique finger impression of a material, is an estimation of the inelastically dissipated light transmitted by the material. The Raman ghasly mark for the material is made by a set out of unambiguous frequencies ( $\lambda_{qs}$ ), related with the collaboration of the episode light with a given cross section vibrational mode  $\nu q$  as an element of the wave vector  $q$ . <sup>14</sup>The Raman shift of a given mode  $\nu q$  is the difference in energy in the in elastically dispersed light as for that of the episode light. The Raman range is a plot of the power of the dispersed light,  $I_s[\delta(1/\lambda_i, s)]$ , as an element of the Raman shift  $\Delta(1/\lambda_i, s)$ , which is given by

$$\Delta(1/\lambda_i, s) = 107\lambda_s - 107\lambda_i, \quad (1)$$

where  $\lambda_i(\lambda_s)$  is the frequency of the occurrence (dispersed) light given in nm and  $\Delta(1/\lambda_i, s)$  is the wavenumber given in units of  $\text{cm}^{-1}$  ( $1\text{eV} = 8065\text{cm}^{-1}$ ). Raman spectroscopy employs  $\text{cm}^{-1}$  as an energy, as is noted. The elementary excitation of a particular mode  $q$  of the material, which is known as a Raman active mode, is represented by the peak of the Raman spectra at  $(1/i, s=q)$ . <sup>15</sup>The plot of  $I_s[\delta(1/\lambda_i, s)]$  is created by a Raman spectrometer, which is typically made by a light scattering grinding and a charged coupled gadget (CCD) camera. The spectrometer software converts the CCD pixel position into " $(1/i, s)$  in  $\text{cm}^{-1}$ ," resulting in the  $I_s[(1/i, s)]$  plot, as the grating scatters the scattered light in a different direction toward the CCD. In Fig., examples are provided. 1, where the  $s_i$  peak would be seen at almost zero Raman shift; however, a notch filter blocks elastic scattering, while the other peaks at  $s_i$  make up the materials' Raman signature.

Fig 1



BERNAS H., Carbon, 44 (2006), 2694.

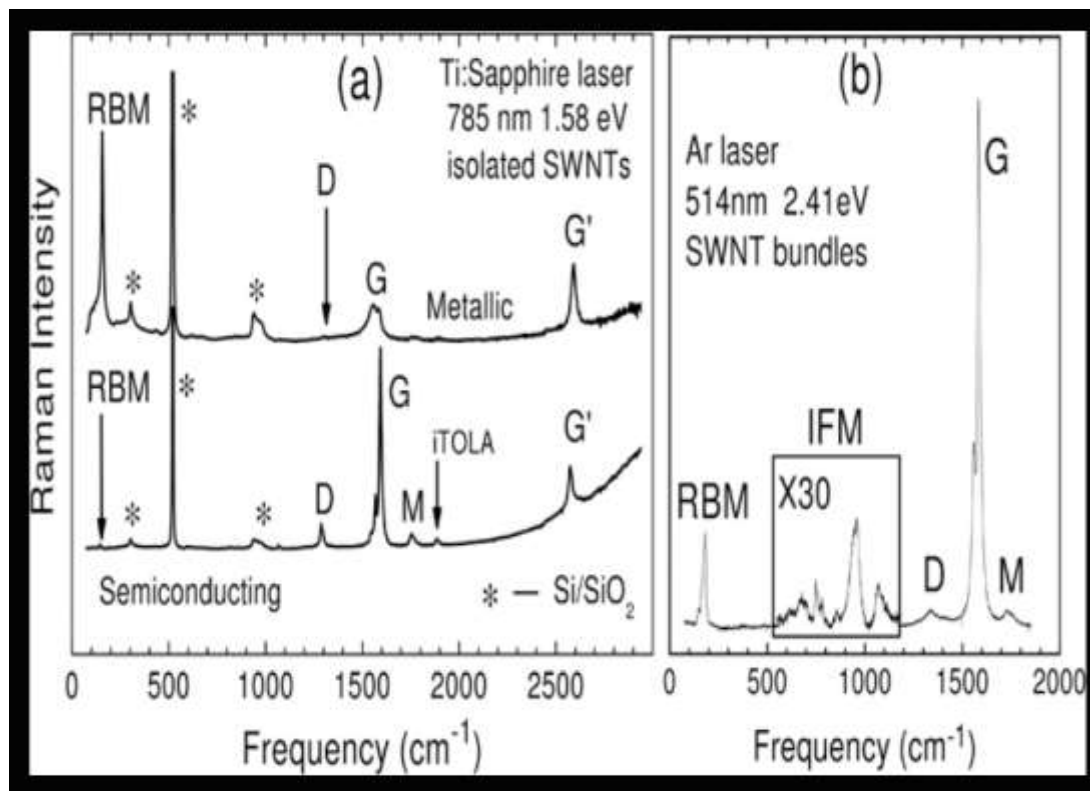
<sup>13</sup> TAKEDA N., MURAKOSHI K., Anal Bioanal Chem., 388 (2007), 103.

<sup>14</sup> R. Ramasubramaniam, J. Chen, and H. Liu, "Homogeneous carbon nanotube/polymer composites for electrical applications," Appl. Phys. Lett. 83, 2928–2930 (2003).

<sup>15</sup> R. Ramasubramaniam, J. Chen, and H. Liu, "Homogeneous carbon nanotube/polymer composites for electrical applications," Appl. Phys. Lett. 83, 2928–2930 (2003).

Exemplary Raman spectra, ascending to descend: amorphous carbon grown by chemical vapor deposition, pristine graphene, highly oriented paralytic graphite (HOPG), single-wall carbon nanotubes (SWNTs), graphene damaged by ion bombardment, and SWNHs. Proven are the spiral breathing modes (RBMs), the imperfection incited tops (D, D' also, the mix D+D'), the G mode, and the hints G' (or on the other hand 2D) and 2G. Replicated with consent from Dresselhaus et al., *Lett Nano.* 10, 751–758 (2010).<sup>16</sup> Copyright, American Chemical Society, 2010.

Fig 2



Carbon nanotube spectra in the Raman range: a) deposition of isolated carbon nanotubes on a substrate made of oxidized silicon (Si/SiO<sub>2</sub>). The spectrum on the top represents a metallic SWNT, while the spectrum on the bottom represents a semiconducting SWNT<sup>17</sup>. Permission granted by Dresselhaus et al., *J. Phys. Chem. C* 111, 17887-17893 (2007).<sup>241</sup> Copyright 2007 American Synthetic Culture. (b) Sample of bundled SWNT. In order to bring out the minuscule intensity peaks, the inset labeled IFM (intermediate frequency modes) has its intensity increased by thirty percent. The peaks of the Si/SiO<sub>2</sub> substrate are marked with a "\*", and the primary Raman features of SWNTs are labeled. Permission granted by Dresselhaus et al., *Philos. Trans. A Math. Phys. Eng. Sci.* 362, 2311–2336 (2004).<sup>242</sup> Royal Society.

### Applications of Raman

**Spectroscopy to Characterize Carbon Nanotubes** The first general aspect of using Raman spectroscopy to characterize carbon nanotubes is the classification of nanotubes into two categories: (1) small diameter few-walls carbon nanotubes (SWNT) and double-wall (DWNT) with smaller diameter tubes below 2 nm; and (2) larger diameter tubes (dt>2 nm) with many walls, specifically multi-wall carbon nanotubes. The chiral vector is defined by the two integers (n,m)<sup>18</sup> in case (1), where the specific SWNT structure can be distinguished by the diameter (dt) and the chiral angle (θ).

<sup>16</sup> A. R. T. Nugraha, E. H. Hasdeo, G. D. Sanders, C. J. Stanton, and R. Saito, "Origin of coherent G-band phonon spectra in single-wall carbon nanotubes," *Phys. Rev. B* 91, 045406 (2015).

<sup>17</sup> A. Bianco, K. Kostarelos, C. D. Partidos, and M. Prato, "Biomedical applications of functionalised carbon nanotubes," *Chem. Commun.* 7, 571–577 (2005).

<sup>18</sup> R. Saito, G. Dresselhaus, and M. S. Dresselhaus, *Physical Properties of Carbon Nanotubes* (Imperial College Press, London, 1998).

In case (2), the properties of many (n,m) SWNTs with a large  $dt$  are too similar to be characterized. As a result, the Raman spectral signature of each (n,m) SWNT or component of a DWNT is distinct for small diameter tubes; however, the results for large diameter tubes are limited to the Raman spectral characteristic of larger diameter tubes ( $dt$ ) or graphene. As a result, the characterization of MWNTs, for instance, is a logical extension of our current focus on the properties of small diameter tubes. See Reference for a comprehensive explanation of the physics underlying carbon nanotube Raman spectra.<sup>19</sup>

### **G and G' (also known as 2D) bands for strain and doping characterization**

In contrast to the RBM, which can only be found in SWNT, the G and G' bands, also known as 2D bands, can be found in all  $sp^2$  carbon structures. These features are unique to applications for two reasons: first, their high frequencies—the G band at 1584  $cm^{-1}$  and the G' band at 2700  $cm^{-1}$ —are the result of a stiff C-C sigma bond and the low mass of the carbon atoms. This is significant because the majority of regular Raman spectrometers can detect shifts of 1.5  $cm^{-1}$  in the G band and 2.7  $cm^{-1}$  in the G' band for every 1% frequency variation. First, the Raman spectra can be used to measure a small change in the Raman shift or linewidths caused by  $^{13}C$  isotope,  $^{122}$  strain, or doping; Second, because metallic  $sp^2$  structures have a strong electron-phonon coupling for a phonon, Raman spectroscopy can be used to precisely measure the Fermi level position. In this section, we will discuss these two effects.<sup>20</sup>

### **Imaging Of Samples And Applications By Raman Spectroscopy**

Raman imaging, in which the Raman intensity of a phonon mode is plotted as a function of the two-dimensional position (X,Y) of the sample or device surface, is one of the useful information provided by Raman spectroscopy. A Z-scan can also be used to create three-dimensional images, but this is less common because selectivity and resolution are not optimal along the direction in which the laser beam propagates, depending on the focusing geometry. The hyper spectra are typically obtained by raster scanning the laser in the sample or device and obtaining one spectrum for each point. Because it carries all of the spectral information at each point in the sample or device, hyper-spectral imaging is much more informative than standard microscopy imaging. In this segment, we examine how we can utilize Raman spectroscopy imaging for portraying tests and the gadgets, tending to miniature Raman in Sec. Section and nano-Raman IV B, and arguing in favour of Raman imaging by contrasting its results with those of other imaging methods in Sec.<sup>21</sup>

### **Nano-Raman spectroscopy imaging**

A tip-enhanced Raman spectroscopy (TERS) system is referred to as a nano-Raman system while a conventional Raman system based on a microscope is known as a micro-Raman system. By scanning a plasmatic Nano antenna on the sample and extracting information from the near-field of light, the Nano-Raman system surpasses the resolution that is required by the light diffraction limit. Surface-upgraded Raman spectroscopy (SERS) is one of the most well-known strategies by utilizing the spatially restricted close field.<sup>22</sup> Nevertheless, SWNTs became a prototype material for the advancement of TERS, which is a variation of SERS in which the plasmatic, local enhancement of the near-field is controlled by a scanning probe microscopy (SPM) system.<sup>192,193</sup> The benefit of TERS is that TERS significantly improves the spatial resolution of Raman images. In fact, SERS has been applied to carbon nanotubes.<sup>186–191</sup> However, due to the sharp resonance Raman effect in the

<sup>19</sup> A. Jorio, M. S. Dresselhaus, R. Saito, and G. Dresselhaus, *Raman Spectroscopy in Graphene Related Systems* (Wiley-VCH Verlag GmbH & Co KGaA, Weinheim, 2010), p. 368.

<sup>20</sup> G. Duesberg, I. Loa, M. Burghard, K. Syassen, and S. Roth, "Polarized Raman spectroscopy on isolated single-wall carbon nanotubes," *Phys. Rev. Lett.* 85, 5436 (2000).

<sup>21</sup> V. Hadjiev, M. Iliev, S. Arepalli, P. Nikolaev, and B. Files, "Raman scattering test of single-wall carbon nanotube composites," *Appl. Phys. Lett.* 78, 3193–3195 (2001).

<sup>22</sup> M. A. Pimenta, G. Dresselhaus, M. S. Dresselhaus, L. G. Cançado, A. Jorio, and R. Saito, "Studying disorder in graphite-based systems by Raman spectroscopy," *Phys. Chem. Chem.*

one-dimensional Although resolution down to the subnanometer scale has already been achieved, TERS offers Raman imaging with a typical spatial resolution of less than 10 nm.<sup>23</sup>

### **Conclusions and Perspectives**

Raman spectroscopy in carbon nanotubes has undergone extensive research over the past two decades and is now mature enough to be used in applications. In this paper, we highlighted the use of Raman spectroscopy to aid in the development of carbon nanotube applications, including a few references from the writing that ranged from materials science to biotechnology. Our initial focus was on the well-established relationships between the most prominent Raman features—the RBM, D, G, and G' bands—and other external factors such as strain, doping, the presence of defects, and interactions with the environment. For ready-to-use protocols, equations, fitting parameters, and observed parameter ranges were provided. Then we discussed how Raman spectroscopy was used to characterise the synthesis, selective sorting, doping, strain, and defects at the end of carbon fibres. Finally, we discussed how micro- and Nano-Raman imaging is superior to standard microscopy because it incorporates functional information. We also discussed other advanced techniques that can be used to improve Raman spectroscopy's ability to describe materials and devices.<sup>24</sup>

The use of Raman spectroscopy not only to characterize materials and devices that will then be used independently of the Raman effect, but also as the device's operating protocol, poses a challenge to this field. Raman spectroscopy will be used to read carbon nanotubes as optical devices, and the Raman spectrum will be used as a functional indicator, such as for strain, doping, and environmental condition sensors. The method is mature enough for this type of work, and lasers and detectors are becoming more powerful and affordable, allowing for new, disruptive innovations.<sup>25</sup>

### **References**

1. Dresselhaus M.S., Dresselhaus G., Jorio A., Souza Filho A.G., Pimenta M.A., Saito D.R., *Acc. Chem. Res.*, 35 (2002), 1070.
2. Y.-P. Sun, K. Fu, Y. Lin, And W. Huang, "Functionalized Carbon Nanotubes: Properties And Applications," *Acc. Chem. Res.* 35, 1096–1104 (2002).
3. M. Endo, M. S. Strano, And P. M. Ajayan, "Potential Applications Of Carbon Nanotubes," In *Carbon Nanotubes* (Springer, 2007), Pp. 13–62.
4. A. Jorio, M. S. Dresselhaus, And G. Dresselhaus, *Carbon Nanotubes: Advanced Topics In The Synthesis, Structure, Properties And Applications*, Topics In Applied Physics Vol. 111 (Springer-Verlag, Berlin, 2008), P. 720.
5. L. Hu, D. S. Hecht, And G. Gruner, "Carbon Nanotube Thin Films: Fabrication, Properties, And Applications," *Chem. Rev.* 110, 5790–5844 (2010).
6. Zhang H.B., Lin G.D., Zhou Z.H., Dong X., Chen T., *Carbon*, 40 (2002), 2429.
7. Grimm D., Grüneis A., Kramberger C., Rummeli M., Gemming T., Büchner B., Barreiro A., Kuzmany H., Pfeiffer R., Pichler T., *Chem. Phys. Lett.*, 428 (2006), 416.
8. Kuzmany H., Plank W., Hulman M., Kramberger C., Grüneis A., Pichler T., Peterlik H., Kataura H., Achiba Y., *Eur. Phys. J. B*, 22 (2001), 307.
9. Antunes E.F., Lobo A.O., Corat E.J., Trava-Airoldi V.J., Martin A.A., Verissimo C., *Carbon*, 44 (2006), 2202.
10. Kürti J., Kuzmany H., Burger B., Hulman M., Winter J., Kresse G., *Synth. Metals*, 103 (1999), 2508
11. Ritter U., Scharff P., Siegmund C., Dmytrenko O.P., Kulish N.P., Prylutsky Yu.I.,

<sup>23</sup> J. Kürti, V. Zólyomi, A. Grüneis, and H. Kuzmany, "Double resonant Raman phenomena enhanced by van Hove singularities in single-wall carbon nanotubes," *Phys. Rev. B* 65, 165433 (2002).

<sup>24</sup> J. Kürti, V. Zólyomi, A. Grüneis, and H. Kuzmany, "Double resonant Raman phenomena enhanced by van Hove singularities in single-wall carbon nanotubes," *Phys. Rev. B* 65, 165433 (2002).

<sup>25</sup> M. S. Dresselhaus, G. Dresselhaus, and A. Jorio, "Raman spectroscopy of carbon nanotubes in 1997 and 2007," *J. Phys. Chem. C* 111, 17887–17893 (2007).

12. Belyi N.M., Gubanov V.A., Komarova L.I., Lizunova S.V., Poroshin V.G., Shlapatskaya V.V., Bernas H., Carbon, 44 (2006), 2694.
13. Takeda N., Murakoshi K., Anal Bioanal Chem., 388 (2007), 103.
14. R. Ramasubramaniam, J. Chen, And H. Liu, "Homogeneous Carbon Nanotube/Polymer Composites For Electrical Applications," Appl. Phys. Lett. 83, 2928–2930 (2003).
15. . R. T. Nugraha, E. H. Hasdeo, G. D. Sanders, C. J. Stanton, And R. Saito, "Origin Of Coherent G-Band Phonon Spectra In Single-Wall Carbon Nanotubes," Phys. Rev. B 91, 045406 (2015).
16. Bianco, K. Kostarelos, C. D. Partidos, And M. Prato, "Biomedical Applications Of Functionalised Carbon Nanotubes," Chem. Commun. 7, 571–577 (2005).
17. R. Saito, G. Dresselhaus, And M. S. Dresselhaus, Physical Properties Of Carbon Nanotubes (Imperial College Press, London, 1998).
18. A. Jorio, M. S. Dresselhaus, R. Saito, And G. Dresselhaus, Raman Spectroscopy In Graphene Related Systems (Wiley-Vch Verlag Gmbh & Co Kga, Weinheim, 2010), P. 368.
19. G. Duesberg, I. Loa, M. Burghard, K. Syassen, And S. Roth, "Polarized Raman Spectroscopy On Isolated Single-Wall Carbon Nanotubes," Phys. Rev. Lett. 85, 5436 (2000).
20. V. Hadjiev, M. Iliev, S. Arepalli, P. Nikolaev, And B. Files, "Raman Scattering Test Of Single-Wall Carbon Nanotube Composites," Appl. Phys. Lett. 78, 3193–3195 (2001).
21. M. A. Pimenta, G. Dresselhaus, M. S. Dresselhaus, L. G. Cançado, A. Jorio, And R. Saito, "Studying Disorder In Graphite-Based Systems By Raman Spectroscopy," Phys. Chem. Chem.
22. J. Kürti, V. Zólyomi, A. Grüneis, And H. Kuzmany, "Double Resonant Raman Phenomena Enhanced By Van Hove Singularities In Single-Wall Carbon Nanotubes," Phys. Rev. B 65, 165433 (2002).
23. J. Kürti, V. Zólyomi, A. Grüneis, And H. Kuzmany, "Double Resonant Raman Phenomena Enhanced By Van Hove Singularities In Single-Wall Carbon Nanotubes," Phys. Rev. B 65, 165433 (2002).
24. M. S. Dresselhaus, G. Dresselhaus, And A. Jorio, "Raman Spectroscopy Of Carbon Nanotubes In 1997 And 2007," J. Phys. Chem. C 111, 17887–17893 (2007).
25. <https://pubs.aip.org/aip/jap/article/129/2/021102/1025611/Raman-spectroscopy-for-carbon-nanotube>